

Research Article

Photocatalytic Ethanol Oxidative Dehydrogenation over Pt/TiO₂: Effect of the Addition of Blue Phosphors

J. J. Murcia,¹ M. C. Hidalgo,¹ J. A. Navío,¹ V. Vaiano,² P. Ciambelli,^{2,3} and D. Sannino^{2,3}

¹Instituto de Ciencia de Materiales de Sevilla (ICMS), Consejo Superior de Investigaciones Científicas CSIC, Universidad de Sevilla, Américo Vespucio 49, 41092 Sevilla, Spain

²Department of Industrial Engineering, University of Salerno, Via Ponte Don Melillo, 84084 Fisciano, Italy

³Nano Mates, Research Centre for Nanomaterials and Nanotechnology at Salerno University, University of Salerno, Via Ponte Don Melillo, 84084 Fisciano, Italy

Correspondence should be addressed to D. Sannino, dsannino@unisa.it

Received 16 July 2011; Accepted 28 August 2011

Academic Editor: Shifu Chen

Copyright © 2012 J. J. Murcia et al. This is an open access article distributed under the Creative Commons Attribution License, which permits unrestricted use, distribution, and reproduction in any medium, provided the original work is properly cited.

Ethanol oxidative dehydrogenation over Pt/TiO₂ photocatalyst, in the presence and absence of blue phosphors, was performed. The catalyst was prepared by photodeposition of Pt on sulphated TiO₂. This material was tested in a gas-solid photocatalytic fluidized bed reactor at high illumination efficiency. The effect of the addition of blue phosphors into the fluidized bed has been evaluated. The synthesized catalysts were extensively characterized by different techniques. Pt/TiO₂ with a loading of 0.5 wt% of Pt appeared to be an active photocatalyst in the selective partial oxidation of ethanol to acetaldehyde improving its activity and selectivity compared to pure TiO₂. In the same way, a notable enhancement of ethanol conversion in the presence of the blue phosphors has been obtained. The blue phosphors produced an increase in the level of ethanol conversion over the Pt/TiO₂ catalyst, keeping at the same time the high selectivity to acetaldehyde.

1. Introduction

The selective oxidation of alcohols is one of the most important reactions in organic chemistry. The conversion of primary alcohols to aldehydes is very important for the synthesis of fine chemicals such as fragrances or food additives [1–6]. There is a great industrial interest to convert low alcohols into useful organic intermediates or products, that is, ethene, diethyl ether, or acetaldehyde [7]. Ethanol serves as a feedstock for acetaldehyde production by oxidative dehydrogenation over pure or mixed oxide catalysts [8–10]. Acetaldehyde is an important intermediary in organic syntheses, and this compound is normally obtained by catalytic ethanol partial oxidation [11, 12]. The catalytic oxidation of ethanol has generally been investigated in order to develop catalysts that maximize products, such as acetaldehyde or acetic acid, and minimize production of deep oxidation reactions [11].

Different supported metals, such as Mo, Fe, Co, Ni, Cu, Ag, V, and Au, has been studied in the current literature for

the reaction of partial oxidation of ethanol by thermal catalysis [11–18]. It is important to note that the selective oxidation of alcohols to either aldehydes or acid in the presence of a noble metal catalyst is of simple work-up procedure, shows a wide applicability to various alcohols, and is an attractive, environment-friendly process [19, 20].

On the other hand, heterogeneous photocatalysis using semiconductor oxides has demonstrated to be very effective in the oxidation of different organic compounds. The heterogeneous photocatalysis based on TiO₂ is an interesting alternative because this oxide is an effective, photostable, reusable, inexpensive, nontoxic, and easily available catalyst [21]. In the past, the majority of the research in the field of photocatalysis was focused on the use of TiO₂ photocatalysts for the purification of water or gas atmospheres from environmental contaminants [22, 23]. However, partial photocatalytic oxidation in the gas phase has recently attracted great interest due to the high potential of this technique in green chemistry [24]. Metal deposition on TiO₂ has been intensively studied

as a means of reducing electron/hole recombination and enhancing efficiencies of TiO_2 in the photocatalytic degradation of organic compounds [25]. Pt deposited on TiO_2 has been reported to improve [26–31], be detrimental [29, 32], or have negligible effects [30] on photocatalysis depending on many different factors.

Chen et al. [32] studied the photocatalytic partial oxidation of ethanol over TiO_2 and Pt/ TiO_2 and found that the selectivity to acetaldehyde (which is more easily oxidized) was enhanced with the platinumization as opposed to the higher formation of acetic acid with bare TiO_2 . These authors explained that loaded on TiO_2 , Pt can accelerate the oxygen reduction process occurring at the cathodic area, thereby diminishing the electron accumulation on the surface of TiO_2 particles. This would accelerate the oxidation rate of alcohols, which, in fact, is controlled by the cathodic reduction of oxygen [32, 33]. This process has been often observed not only for alcohols, but also for other organic compounds. Vorontsov and Dubovitskaya [34] reported also up to a two times increase in the rate of ethanol photooxidation at various Pt loadings.

In previous papers regarding the oxidative dehydrogenation of organic compounds using fluidized bed photoreactors [17, 35–37], it has been evinced that UV light does not penetrate in the reactor core volume, since it is mostly absorbed by the catalyst circulating near the irradiated reactor windows within few millimetres [17]. To improve photon transfer in the reactor core volume, the reactor thickness has to be reduced, and, moreover, it is possible to mix the photocatalyst with emitting phosphorescent particles as light carriers, known generally as phosphors. Recently, some of us have reported that the addition of phosphors into a fluidized bed has, therefore, resulted in about doubling of the catalytic surface totally irradiated [17], allowing a considerably increase of the photocatalytic activity. In this paper, the selective partial oxidation of ethanol to acetaldehyde over Pt/ TiO_2 photocatalyst was studied. The photocatalytic reactions were carried out in a gas-solid photocatalytic fluidized bed reactor. The study of the effect of the addition of blue phosphors into the fluidized bed was also attempted.

2. Experimental

2.1. Synthesis Procedure. TiO_2 used as starting material was prepared by the hydrolysis of titanium tetraisopropoxide (Aldrich, 97%) in isopropanol solution (1.6 M) by the slow addition of distilled water (volume ratio isopropanol/water 1 : 1). Afterward, the generated precipitate was filtered and dried at 110°C overnight. The powders thus obtained were then sulphated by immersion in 1 M sulphuric acid solution for 1 h and calcinated at 650°C for 2 h. Sulphate treatment was carried out for two reasons. On one hand, previous results have shown that sulphate pretreatment stabilizes anatase phase up to high temperatures and protects surface area against sintering [38]. On the other hand, at the calcination temperature of 650°C , the elimination of sulphate groups promotes the creation of high number of oxygen vacancies,

which have been reported as preferential sites for Pt adsorption [39].

Photodeposition of platinum was performed over the calcined TiO_2 powder using hexachloroplatinic acid (H_2PtCl_6 , Aldrich 99.9%) as metal precursor. Under an inert atmosphere (N_2), a suspension of TiO_2 in distilled water containing isopropanol (Merck 99.8%) which acts as sacrificial donor was prepared. Then, the appropriate amount of H_2PtCl_6 to obtain a nominal platinum loading of 0.5% weight total to TiO_2 was added. Final pH of the suspensions was 3. Photodeposition of platinum was then performed by illuminating the suspension during 120 min with an Osram Ultra-Vitalux lamp (300 W) with a sun-like radiation spectrum and a main emission line in the UVA range at 365 nm. The intensity of the lamp was 140 W/m^2 . After photodeposition, the powders were recovered by filtration and dried at 110°C overnight.

Blue phosphors (model RL-UV-B-Y; Excitation Wavelength: 365 nm; Emission Wavelength: 440 nm; particles diameter: 5–10 μm) were provided by DB Chemic. A wide characterization of this material was carried out, and these results are collected in a recent article [17], evidencing that the host crystal structure of the phosphors used in this work is ZnS.

2.2. Characterization Techniques. Crystalline phase composition and degree of crystallinity of the samples were estimated by X-ray diffraction (XRD). XRD patterns were obtained on a Siemens D-501 diffractometer with Ni filter and graphite monochromator using $\text{Cu K}\alpha$ radiation. Crystallite sizes were calculated from the line broadening of the main X-ray diffraction peaks by using the Scherrer equation. Peaks were fitted by using a Voigt function.

Laser Raman spectra of catalyst were obtained at room temperature with a Dispersive MicroRaman (Invia, Renishaw), equipped with 785 nm diode-laser, in the range $100\text{--}2500\text{ cm}^{-1}$ Raman shift.

Light absorption properties of the samples were studied by UV-Vis spectroscopy. The UV-Vis DRS spectra were recorded by a Perkin Elmer spectrometer Lambda 35. Bandgaps values were calculated from the corresponding Kubelka-Munk functions, $F(R_\infty)$, which are proportional to the absorption of radiation, by plotting $(F(R_\infty) \cdot h\nu)^2$ against $h\nu$.

BET surface area and porosity measurements were carried out by N_2 adsorption at 77 K using a Micromeritics ASAP 2010 instrument.

Chemical composition and total platinum content of the samples were determined by X-ray fluorescence spectrometry (XRF) in a Panalytical Axios sequential spectrophotometer equipped with a rhodium tube as the source of radiation. XRF measurements were performed onto pressed pellets (sample included in 10 wt% of wax).

Thermogravimetric analysis (TG-DTG) of the samples was carried out in air flow with a thermobalance (SDT Q600, TA Instruments), in the range $20^\circ\text{C}\text{--}1000^\circ\text{C}$ at heating rate of $10^\circ\text{C}/\text{min}$.

Field emission SEM images were obtained in a Hitachi S-4800 microscope. The samples were dispersed in ethanol

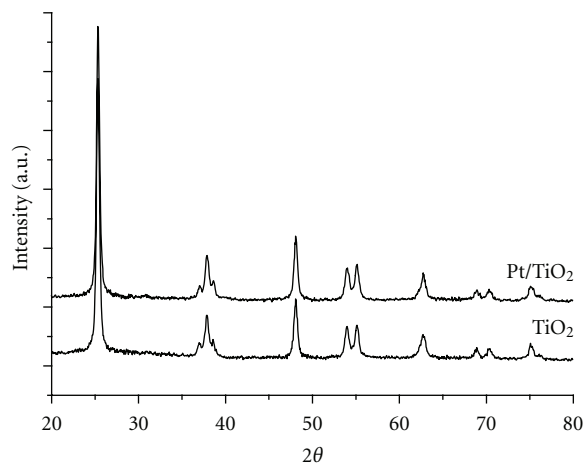


FIGURE 1: XRD patterns for TiO₂ and Pt/TiO₂ photocatalysts.

using an ultrasonicator and dropped on a carbon grid. The platinum particle sizes were evaluated by TEM, in a microscope Philips CM 200.

X-ray photoelectron spectroscopy (XPS) studies were carried out on a Leybold-Heraeus LHS-10 spectrometer, working with constant pass energy of 50 eV. The spectrometer main chamber, working at a pressure $< 2 \times 10^{-9}$ Torr, is equipped with an EA-200 MCD hemispherical electron analyser with a dual X-ray source working with Al K α ($h\nu = 1486.6$ eV) at 120 W and 30 mA. C 1s signal (284.6 eV) was used as internal energy reference in all the experiments. Samples were outgassed in the prechamber of the instrument at 150°C up to a pressure $< 2 \times 10^{-8}$ Torr to remove chemisorbed water.

2.3. Photocatalytic Tests. Photocatalytic tests were carried out with a feeding 30 L/h (STP), at ethanol concentration in the range 0.1–2 vol.%, in helium flow with oxygen/ethanol ratio of 2. Temperature and pressure reaction were 60°C and 1 atm, respectively. Oxygen and helium were fed from cylinders, helium being the carrier gas for ethanol vaporized from a temperature controlled saturator. Different concentrations of ethanol in the reaction feed were obtained by changing temperature and He flow through the saturator. The gas flow rates were measured and regulated by mass flow controllers (Brooks Instrument).

The fluidized bed reactor used in this work was designed for working with a gas flow rate in the range 20–70 L/h (STP) with a Sauter average diameter in the particles size range 50–100 μm , assuring optimal fluidization [17, 35]. It was a two-dimensional reactor with 40 mm \times 6 mm cross-section, 230 mm height pyrex-glass walls, and a bronze filter (mean pores size 5 μm) to provide a uniform distribution of fed gas. In order to decrease the amount of transported particles, an expanding section (50 mm \times 50 mm cross-section at the top) and a cyclone specifically designed [36] are located on the top and at the outlet of the reactor, respectively. The reactor was illuminated by two UVA-LEDs modules (80 \times 50 mm

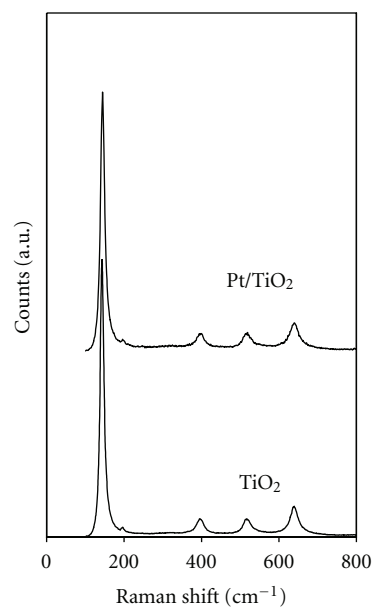


FIGURE 2: Raman spectra of TiO₂ and Pt/TiO₂ photocatalysts.

positioned in front of the reactor pyrex windows (light intensity: 90 mW/cm²). Each module consisted of 40 UV-LEDs emitting at 365 nm (provided by Nichia Corporation). With these illumination conditions, the light pathlength in the photoreactor was about 2 mm. The catalytic bed was composed by 1.2 g of catalyst diluted with 20 g of glass spheres (grain size: 70–110 μm) (Lampugnani Sandblasting HI-TECH).

To optimize the composition of fluidizable solid mixture, photocatalytic tests were also carried out in the presence of blue phosphors. For these tests, the catalytic bed was composed by 1.2 g of catalyst and 1.8 g of blue phosphors diluted with 20 g of glass spheres. In this way, phosphors were fluidized with the catalyst, excited by external UVA-LEDs, and emitted their stored energy in the proximity to the catalyst.

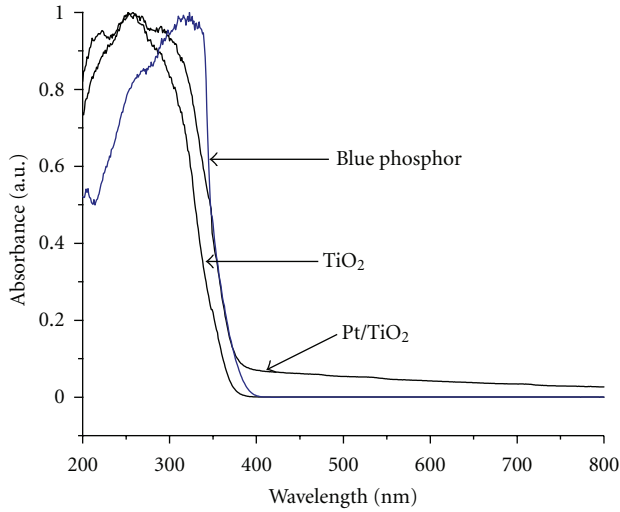
Hereon, the catalytic systems are denoted as Pt/TiO₂ and Pt/TiO₂ + Blue P for the setups without and with phosphors, respectively.

Concentrations of inlet reactants and outlet products were measured by an online mass detector (MS) (Quantra Fourier transform ion cyclotron resonance mass spectrometer, Siemens) and a continuous CO-CO₂ NDIR analyzer (Uras 10, Hartmann and Braun).

Preliminary tests were carried out to check the amount of solid particles elutriated from the reactor by fluidizing the powders for several hours. Elutriation was negligible, confirmed also by the stability of catalytic activity during irradiation time in the photocatalytic tests. In addition, experimental tests to check the fluidization properties were realized, both in the presence and absence of phosphors. These tests showed that the expansion of fluidized bed was the same in both cases, evidencing that the fluidization regime did not change in the presence of phosphors.

TABLE 1: Summary of characterization results.

Catalyst	S_{BET} (m ² /g)	Anatase crystallite size (nm)	S (SO ₃ %)	nOH/g (mol/g)	nOH/m ² (mol/m ²)	Ethanol adsorption (mmol/g)
TiO ₂	58.3	20	0.52	6.6 E-4	8.8 E-6	0.5
Pt/TiO ₂	59.0	21	0.39	1.2 E-3	2.1 E-5	1.6

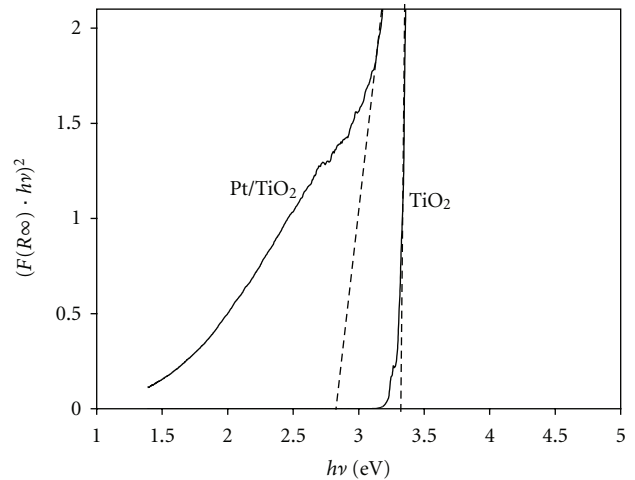
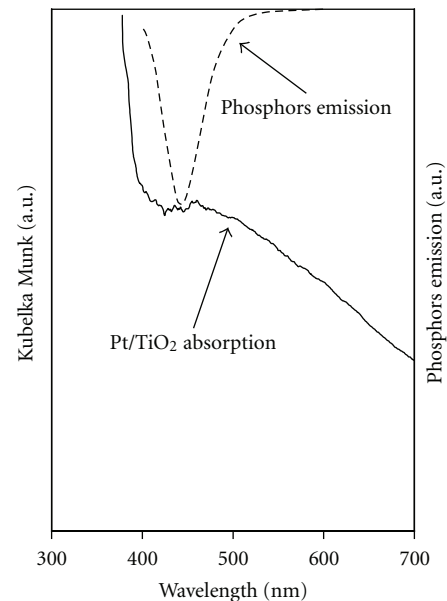
FIGURE 3: UV-Vis DRS spectra for TiO₂ and Pt/TiO₂ photocatalysts compared with phosphors emission.

3. Results and Discussion

3.1. Characterization of the Catalysts. The XRD patterns (Figure 1) and Raman spectra (Figure 2) for sulphated TiO₂ and Pt/TiO₂ photocatalyst showed that anatase is the only crystalline phase present in these samples. The stabilization of anatase phase by sulphate pretreatment of the TiO₂ can be noticed here, as no traces of rutile were found even after the high calcination temperature used (650°C) [38, 40]. No peaks corresponding to platinum was detected by XRD due to the low loading and high dispersion of metal present in the Pt/TiO₂ catalyst. Anatase crystallite sizes of the samples were estimated by the Scherrer equation, and the values are presented in Table 1. As it can be observed, the addition of platinum did not induce any significant change in the anatase crystallite size of TiO₂ (20-21 nm).

Figure 3 shows the UV-Vis DRS spectra for Pt/TiO₂ catalyst and the starting material (sulphated TiO₂). No significant differences between the spectra analyzed are visible for wavelengths below 400 nm in which the characteristic sharp absorption threshold of TiO₂ around 350 nm can be observed. For Pt/TiO₂ catalyst, in the range between 400 and 600 nm, there is the presence of a very broad absorption band probably due to an interaction between platinum surface species and titanium dioxide. Figure 3 shows also the UV-Vis DRS spectrum of blue phosphors; this sample has absorption at wavelength of 320 nm and band gap energy of 3.1 eV.

Differences in the absorption properties of the two catalysts are markedly evinced by plotting $[F(R_{\infty}) * hv]^2$ versus $h\nu$ (Figure 4) and correspond to a decrease in band gap

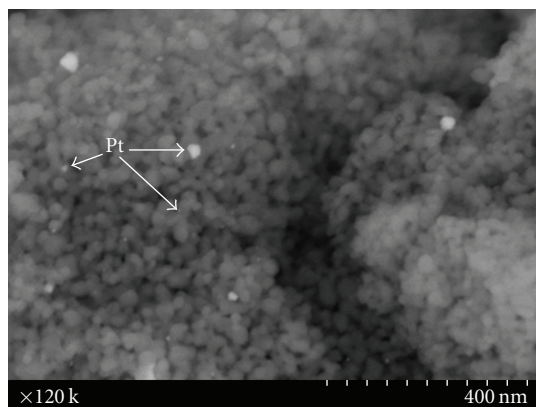
FIGURE 4: Band gap calculus from UV-Vis DRS spectra for TiO₂ and Pt/TiO₂ catalysts.FIGURE 5: Comparison between Pt/TiO₂ absorption and phosphors emission.

energies, from 3.4 eV for TiO₂ to 2.8 eV for Pt/TiO₂ sample. This last value implies that the activation energy can be provided by the energy related to the wavelength emission of the selected phosphors (Figure 5).

BET surface area values for the analyzed samples are given in Table 1. As it can be observed, a little increase in the TiO₂ S_{BET} value was produced by the process of platinum photodeposition.

TABLE 2: XPS results.

Catalysts	Binding energy (eV)		Pt ⁰ (%)	Pt ^{δ+} (%)
	Ti 2p _{3/2}	O 1s		
TiO ₂	458.5	529.8	—	—
Pt/TiO ₂	458.4	529.6	70.2	29.8

FIGURE 6: Selected scanning electron image of Pt/TiO₂ photocatalyst.

Total amount of platinum in the Pt/TiO₂ photocatalyst was calculated by XRF, being 0.41%. This value is close to the nominal content (0.5%) indicating a high yield for the photodeposition process. XRF analysis also showed the presence of sulphur from the sulphate pretreatment even though the amount of this element was low corresponding just to a 0.39%.

Hydroxyls surface densities were evaluated by TG-DTG losses in the temperature range of 180°C–300°C. The analysis revealed that the hydroxyls groups on the surface of the TiO₂ increased with the deposition of Pt. The TG-DTG results (Table 1) also showed that remaining sulphur content on TiO₂ decreased with the addition of platinum, probably due to the synthesis procedure of the Pt/TiO₂ catalyst.

The samples were studied by SEM and TEM to obtain information about Pt particle size and dispersion. A selected SEM micrograph for Pt/TiO₂ catalyst is presented in Figure 6. As it can be clearly observed, platinum particles are quite heterogeneously distributed over the oxide surface with a poor dispersion, and the metal deposits present different sizes. TEM was used to estimate the Pt particle size distribution. One selected micrograph is shown in Figure 7 together with a representation of the metal particle size distribution estimated by counting and measuring particles in a high number of micrographs taken on different areas of the sample. As we can see, Pt particles present a heterogeneous distribution, with the highest number of particles (ca. 35%) being in the range of particle size of 5–6 nm.

XPS studies for TiO₂ and Pt/TiO₂ catalyst were also carried out, and a summary of the obtained results is shown in Table 2. For the platinized sample, it was especially useful to analyze the Pt 4f core level (4f_{7/2} and 4f_{5/2}) (Figure 8).

The region corresponding to Pt peaks may be deconvoluted into two components: one corresponding to Pt⁰ at binding energy of 74.5 eV and an other assigned to a partially oxidised Pt^(δ+) at binding energy of 71.1 eV [41]. In this way, it is possible to make an estimation of the fraction of Pt in the metallic state (Pt⁰) and in the oxidized state (Pt⁽²⁺⁾/Pt⁽⁴⁺⁾). The deconvolution of the peaks as achieved by using the program UNIFIT 2009 [42] and the results are presented in Table 2 and in Figure 8. As it can be seen, the major part of platinum (ca. 70%) is present on the sample as metallic platinum (Pt⁰), while about the 30% of the metal was not totally reduced, and it was still present as oxidized forms (Pt^(δ+)). The oxidation state of Pt particles on the TiO₂ is one of the most important parameters influencing the improvement of the photocatalytic activity of TiO₂ according to many previous reported results [43, 44], being Pt⁰ the state of the metal that appears to provide the highest enhancement of activity.

Regarding the analysis of the O 1s region, a peak located at a binding energy of 529.8 ± 0.2 eV was registered in both samples, corresponding to lattice oxygen in TiO₂, with a broad shoulder at higher binding energies ascribed to surface hydroxyl groups. This later shoulder was more pronounced for the Pt/TiO₂ sample, indicating a higher degree of hydroxylation, in agreement with TG-DTG results. On the other hand, the XPS Ti 2p core level spectra were similar for TiO₂ and Pt/TiO₂ without significant changes in the binding energy of the peaks (458.5 ± 0.1 eV), corresponding to Ti⁴⁺ as the main component.

From XPS data, O/Ti ratios were calculated for sulphated TiO₂ and Pt/TiO₂ samples. For the pure sulphated TiO₂, O/Ti value is 1.70, lower than the stoichiometric value (O/Ti = 2), indicating the presence of oxygen vacancies on the surface of this oxide. It has been reported that sulphated TiO₂ presents a lower O/Ti ratio than nonsulphated TiO₂, which indicates that the amount of oxygen vacancies is higher in the former samples [38]. For Pt/TiO₂ the O/Ti ratio is higher (O/Ti = 1.88), suggesting that the oxygen vacancies are partially annihilated during the photodeposition process.

3.2. Photocatalytic Tests. The evaluation of the photocatalytic activity was carried out by following the reaction of ethanol oxidative dehydrogenation in gas phase. All the photocatalytic tests started feeding the reaction gaseous mixture to the reactor in the dark, until the outlet ethanol concentration reached the equilibrium value, taken as initial value. Therefore, UVA-LEDs were switched on after the establishment of the dark adsorption equilibrium of ethanol on the catalyst surface. No reaction products were observed during or after the ethanol dark adsorption at 60°C, indicating that no selective ethanol oxidation occurs by thermal catalysis in the used operating conditions [17].

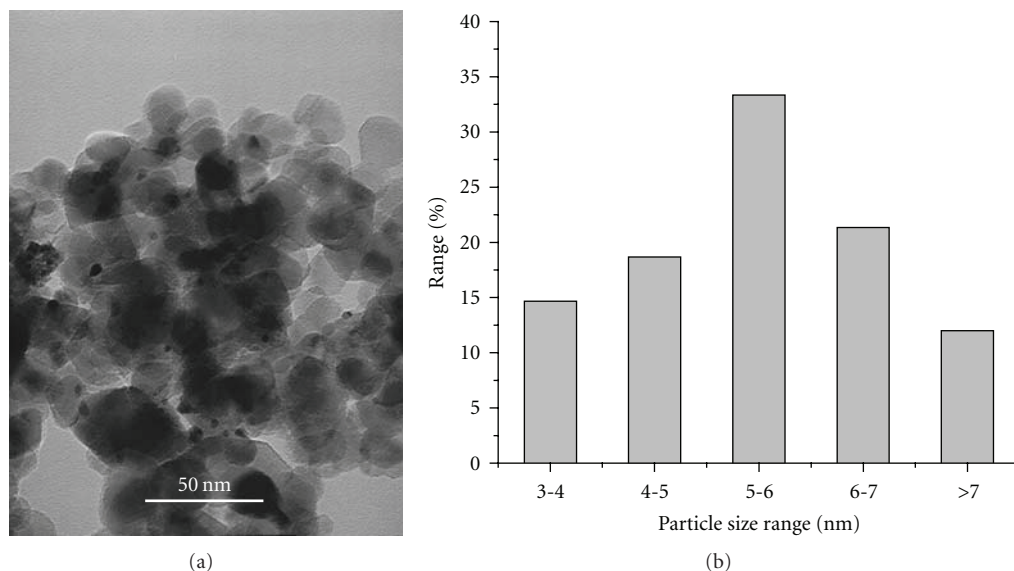


FIGURE 7: Selected transmission electron micrograph and distribution of platinum particle sizes of Pt/TiO₂ photocatalyst.

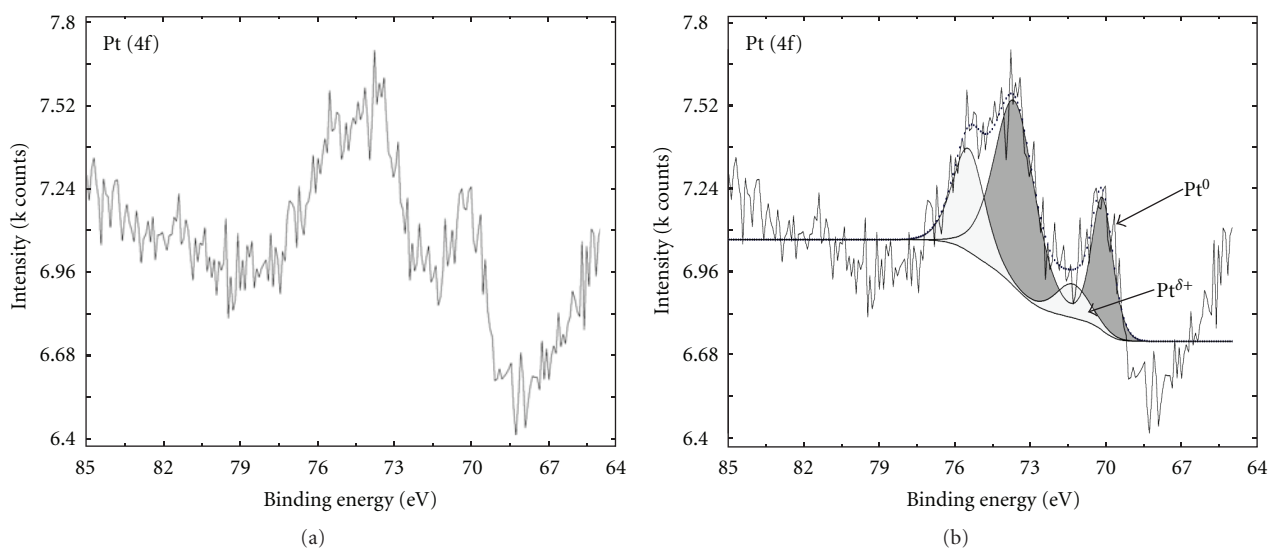


FIGURE 8: XPS Pt 4f core level for Pt/TiO₂ photocatalyst.

The photocatalytic activity of the pure (TiO₂) and platinumized oxide (Pt/TiO₂) in the presence and absence of blue phosphors was evaluated for the reaction of ethanol dehydrogenation at a concentration of 0.2 vol%. Ethanol photocatalytic conversion on Pt/TiO₂ as a function of the ethanol inlet concentration was also investigated. Results are presented in Figure 9. As it can be seen, the photocatalytic activity of TiO₂ is slightly improved by the photodeposition of Pt. Thus, the ethanol conversion increased with the addition of platinum reaching a maximum of about 69% at 0.2 vol% of initial ethanol concentration. At higher ethanol concentration values, conversion progressively decreased going down to 7% for 2 vol% of ethanol. According to MS analysis, acetaldehyde was the main product together with low amounts of CO₂,

ethylene and crotonaldehyde as byproducts which were also detected.

The effect of metal deposition on the photocatalytic activity of TiO₂ has been widely studied [25–30]. Noble metal nanoparticles deposited on the TiO₂ surface are known to act as effective traps for photogenerated electrons due to the formation of a Schottky barrier at the metal-semiconductor contact. These electrons improve the rate of oxygen reduction and inhibit the electron-hole recombination even though the improvement of activity in this work has not been as accused as in other reported literature, being strongly depending on the considered substrate [27–31].

As it is also shown in Figure 9, the addition of blue phosphors notably increased the activity of the Pt/TiO₂ catalyst

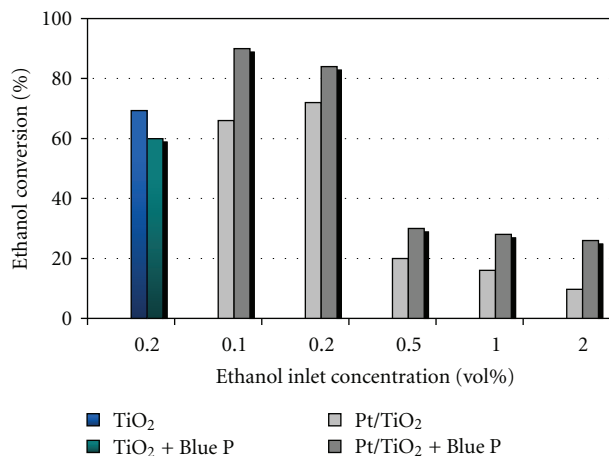


FIGURE 9: Ethanol conversion on Pt/TiO₂ photocatalyst as a function of ethanol inlet concentration.

for all the ethanol concentrations studied. In the same manner then for the tests without phosphors, total ethanol conversion decreased with the increase of ethanol concentration; however, as it has been said, for all ethanol concentrations analyzed, an important improvement of the photocatalytic activity of Pt/TiO₂ catalyst with the addition of phosphors into the fluidized bed can be observed. This is due to the phosphors exploited as light carriers inside the photocatalytic core bed, giving a shorter optical pathlength to the radiation. Moreover, the photoactivity was enhanced, because the suitable phosphors introduced into the system were able to transform 365 nm radiation coming from UV-LEDs into 440 nm emission and able to photoexcited the fraction of photocatalyst in the core reactor volume, otherwise screened by the photocatalyst itself as previously found for V₂O₅/TiO₂ [17].

Blank tests were also carried out under irradiation with the reactor loaded only with phosphors and glass spheres without catalyst showing only negligible ethanol consumption and acetaldehyde production. In this test, the ethanol conversion was less than 2%; therefore, the presence of the specific photocatalyst was necessary for the reaction [17].

In a same way, a blank test with an inlet ethanol concentration of 0.2 vol%, using only sulphated pure TiO₂, phosphors, and glass spheres, was carried out, and we have found an ethanol conversion of 60%. The conversion is lower than that obtained without phosphors, because the phosphors act as screening for UV light decreasing the percentage of TiO₂ effectively irradiated. This result underlines that Pt species are crucial to activate the catalysts at emission wavelength of phosphors.

With an inlet ethanol concentration of 0.2 vol%, the conversion levels for sulphated pure TiO₂, Pt/TiO₂, and Pt/TiO₂ + Blue phosphors corresponded to values of 69%, 72%, and 84%, respectively. At higher initial inlet concentration, the increase in ethanol conversion in the presence of blue phosphors clearly evidenced the photon transfer limitations in the absence of phosphors that are overcome with

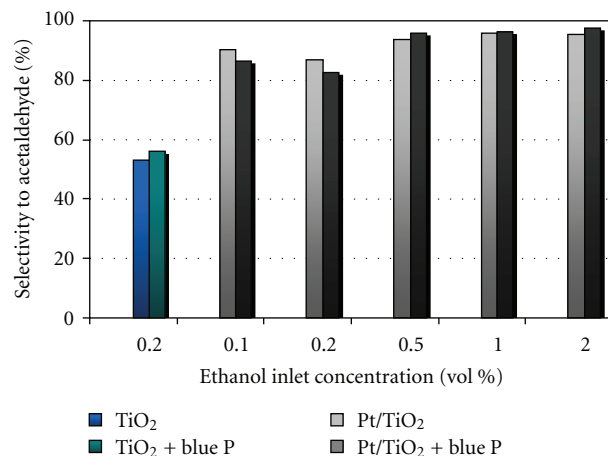


FIGURE 10: Acetaldehyde selectivity as a function of ethanol inlet concentration.

Pt/TiO₂ photocatalyst and able to catch the light emission carried by phosphors.

Selectivity trend for the different systems as a function of ethanol concentration is shown in Figure 10. It can be noticed that addition of Pt to the TiO₂ remarkably increased the selectivity to acetaldehyde at the studied ethanol concentration of 0.2 vol%. On the other hand, the selectivity to acetaldehyde obtained with the Pt/TiO₂ photocatalyst is very similar for the different ethanol concentrations evaluated, and in any case, it is notably higher than the selectivity obtained with the pristine TiO₂.

These results suggest that the reaction mechanism for ethanol conversion follows different pathways when using pure or platinized TiO₂, as it has been already reported by Siemon et al. for different substrates over platinized and non-platinized commercial TiO₂ [31]. A hypothesis on the action of Pt in the reaction mechanism could be related to the already suggested formation of acetaldehydes radicals on TiO₂. In fact, considering that in TiO₂, ethanol is adsorbed as ethoxy specie and the formation of OH radicals under UV irradiation by reaction of hydroxyls with positive holes, the abstraction of hydrogen by the adsorbed ethoxy species results in adsorbed acetaldehyde radicals [29]. Acetaldehyde radical could be transformed into adsorbed acetaldehyde by electron withdrawing by Pt nanoparticles then favouring the desorption of the product.

In the presence of blue phosphors, the main reaction product was also acetaldehyde, and the selectivity to this compound was also much higher than the one obtained with the pure TiO₂. The acetaldehyde selectivity of Pt/TiO₂ catalyst with or without the addition of blue phosphors is very similar, increasing slightly with the ethanol concentration, with values ranging 90%–95%.

4. Conclusions

The ethanol oxidative dehydrogenation in gas phase using sulphated TiO₂ and Pt/TiO₂ as catalysts has been studied.

An efficient photocatalyst, active and selective to acetaldehyde in the ethanol dehydrogenation, can be obtained by modification of TiO₂ by photodeposition of platinum nanoparticles. We can observe that the photocatalytic activity of TiO₂ and selectivity to acetaldehyde can be improved by photodeposition of platinum. In the same way, the effect of the addition of blue phosphors to photocatalytic bed was evaluated. Experimental data evidenced that the presence of phosphors allowed an improving in the photocatalytic activity of Pt/TiO₂, limited by the photon transfer, because a notable increase of ethanol conversion was observed.


Acknowledgments

This research was financed by the Spanish Ministerio Ciencia e Innovación (Project no. CTQ2008-05961-CO2-01) and Junta de Andalucía (Excellence Project no. P06-FQM-1406). J. J. Murcia thanks CSIC for the concession of a JAE grant and for financing the short stay no. 2011ESTCSIC-6717. The authors would like also to thank Lampugnani Sandblasting HI-TECH for the glass spheres utilized in this work.

References

- [1] M. Musawir, P. N. Davey, G. Kelly, and I. V. Kozhevnikov, "Highly efficient liquid-phase oxidation of primary alcohols to aldehydes with oxygen catalysed by Ru-Co oxide," *Chemical Communications*, vol. 9, no. 12, pp. 1414–1415, 2003.
- [2] D. Ramakrishna and B. R. Bhat, "A catalytic process for the selective oxidation of alcohols by copper (II) complexes," *Inorganic Chemistry Communications*, vol. 14, no. 5, pp. 690–693, 2011.
- [3] S. Velusamy, A. Srinivasan, and T. Punniyamurthy, "Copper(II) catalyzed selective oxidation of primary alcohols to aldehydes with atmospheric oxygen," *Tetrahedron Letters*, vol. 47, no. 6, pp. 923–926, 2006.
- [4] R. A. Sheldon and J. K. Kochi, *Metal-Catalyzed Oxidation of Organic Compounds*, Academic Press, New York, NY, USA, 1981.
- [5] M. Hudlicky, *Oxidations in Organic Chemistry*, An American Chemical Society Publication, Washington, DC, USA, 1990.
- [6] U. R. Pillai and E. Sahle-Demessie, "Selective oxidation of alcohols in gas phase using light-activated titanium dioxide," *Journal of Catalysis*, vol. 211, no. 2, pp. 434–444, 2002.
- [7] A. A. Abd El-Raady, N. E. Fouad, M. A. Mohamed, and S. A. Halawy, "Effect of the preparation method of Al-Mg-O catalysts on the selective decomposition of ethanol," *Monatshfte fur Chemie*, vol. 133, no. 10, pp. 1351–1361, 2002.
- [8] A. Yee, S. J. Morrison, and H. Idriss, "A study of the reactions of ethanol on CeO₂ and Pd/CeO₂ by steady state reactions, temperature programmed desorption, and in situ FT-IR," *Journal of Catalysis*, vol. 186, no. 2, pp. 279–295, 1999.
- [9] W. Zhang, A. Desikan, and S. T. Oyama, "Effect of support in ethanol oxidation on molybdenum oxide," *Journal of Physical Chemistry*, vol. 99, no. 39, pp. 14468–14476, 1995.
- [10] S. A. Halawy and M. A. Mohamed, "The effect of different ZnO precursors on the catalytic decomposition of ethanol," *Journal of Molecular Catalysis A*, vol. 98, no. 2, pp. L63–L68, 1995.
- [11] R. Tesser, V. Maradei, M. Di Serio, and E. Santacesaria, "Kinetics of the oxidative dehydrogenation of ethanol to acetaldehyde on V₂O₅/TiO₂-SiO₂ catalysts prepared by grafting," *Industrial and Engineering Chemistry Research*, vol. 43, no. 7, pp. 1623–1633, 2004.
- [12] E. A. Sales, T. R.O. De Souza, R. C. Santos, and H. M.C. Andrade, "N₂O decomposition coupled with ethanol oxidative dehydrogenation reaction on carbon-supported copper catalysts promoted by palladium and cobalt," *Catalysis Today*, vol. 107–108, pp. 114–119, 2005.
- [13] H. H. Tseng, M. Y. Wey, and C. H. Fu, "Carbon materials as catalyst supports for SO₂ oxidation: catalytic activity of CuO-AC," *Carbon*, vol. 41, no. 1, pp. 139–149, 2003.
- [14] S. T. Oyama and W. Zhang, "True and spectator intermediates in catalysis: the case of ethanol oxidation on molybdenum oxide as observed by in situ laser Raman spectroscopy," *Journal of the American Chemical Society*, vol. 118, no. 30, pp. 7173–7177, 1996.
- [15] H. Nair, J. E. Gatt, J. T. Miller, and C. D. Baertsch, "Mechanistic insights into the formation of acetaldehyde and diethyl ether from ethanol over supported VO_x, MoO_x, and WO_x catalysts," *Journal of Catalysis*, vol. 279, no. 1, pp. 144–154, 2011.
- [16] E. Santacesaria, A. Sorrentino, R. Tesser, M. Di Serio, and A. Ruggiero, "Oxidative dehydrogenation of ethanol to acetaldehyde on V₂O₅/TiO₂-SiO₂ catalysts obtained by grafting vanadium and titanium alkoxides on silica," *Journal of Molecular Catalysis A: Chemical*, vol. 204–205, pp. 617–627, 2003.
- [17] P. Ciambelli, D. Sannino, V. Palma, V. Vaiano, and R. S. Mazzei, "Intensification of gas-phase photooxidative dehydrogenation of ethanol to acetaldehyde by using phosphors as light carriers," *Photochemical and Photobiological Sciences*, vol. 10, pp. 414–418, 2011.
- [18] C. Della Pina, E. Falletta, L. Prati, and M. Rossi, "Selective oxidation using gold," *Chemical Society Reviews*, vol. 37, no. 9, pp. 2077–2095, 2008.
- [19] P. Korovchenko, C. Donze, P. Gallezot, and M. Besson, "Oxidation of primary alcohols with air on carbon-supported platinum catalysts for the synthesis of aldehydes or acids," *Catalysis Today*, vol. 121, no. 1–2, pp. 13–21, 2007.
- [20] C. H. Christensen, B. Jørgensen, J. Rass-Hansen et al., "Formation of acetic acid by aqueous-phase oxidation of ethanol with air in the presence of a heterogeneous gold catalyst," *Angewandte Chemie—International Edition*, vol. 45, no. 28, pp. 4648–4651, 2006.
- [21] A. Haarstrick, O. M. Kut, and E. Heinzle, "TiO₂-assisted degradation of environmentally relevant organic compounds in wastewater using a novel fluidized bed photoreactor," *Environmental Science and Technology*, vol. 30, no. 3, pp. 817–824, 1996.
- [22] A. Sirisuk, C. G. Hill Jr., and M. A. Anderson, "Photocatalytic degradation of ethylene over thin films of titania supported on glass rings," *Catalysis Today*, vol. 54, no. 1, pp. 159–164, 1999.
- [23] D. M. Blake, *Bibliography of Work on the Photocatalytic Removal of Hazardous Compounds from Water and Air Update Number 2 to October 1996*, NREL/TP-430-22197, National Renewable Energy Laboratory, Golden, Colo, USA, 1996.
- [24] J. M. Herrmann, C. Duchamp, M. Karkmaz et al., "Environmental green chemistry as defined by photocatalysis," *Journal of Hazardous Materials*, vol. 146, no. 3, pp. 624–629, 2007.
- [25] F. Denny, J. Scott, K. Chiang, W. Y. Teoh, and R. Amal, "Insight towards the role of platinum in the photocatalytic mineralisation of organic compounds," *Journal of Molecular Catalysis A: Chemical*, vol. 263, no. 1–2, pp. 93–102, 2007.
- [26] M. C. Hidalgo, M. Maicu, J. A. Navío, and G. Colón, "Study of the synergic effect of sulphate pre-treatment and platinisation on the highly improved photocatalytic activity of TiO₂," *Applied Catalysis B: Environmental*, vol. 81, no. 1–2, pp. 49–55, 2008.

- [27] K. Chiang, T. M. Lim, C. C. Lee, and L. Tsen, "Photocatalytic degradation and mineralization of bisphenol A by TiO₂ and platinumized TiO₂," *Applied Catalysis A: General*, vol. 261, no. 2, pp. 225–237, 2004.
- [28] M. Lindner, J. Theurich, and D. W. Bahnemann, "Photocatalytic degradation of organic compounds: accelerating the process efficiency," *Water Science and Technology*, vol. 35, no. 4, pp. 79–86, 1997.
- [29] J. C. Crittenden, J. Liu, D. W. Hand, and D. L. Perram, "Photocatalytic oxidation of chlorinated hydrocarbons in water," *Water Research*, vol. 31, no. 3, pp. 429–438, 1997.
- [30] H. M. Coleman, K. Chiang, and R. Amal, "Effects of Ag and Pt on photocatalytic degradation of endocrine disrupting chemicals in water," *Chemical Engineering Journal*, vol. 113, no. 1, pp. 65–72, 2005.
- [31] U. Siemon, D. Bahnemann, J. J. Testa, D. Rodríguez, M. I. Litter, and N. Bruno, "Heterogeneous photocatalytic reactions comparing TiO₂ and Pt/TiO₂," *Journal of Photochemistry and Photobiology A: Chemistry*, vol. 148, no. 1-3, pp. 247–255, 2002.
- [32] J. Chen, D. F. Ollis, W. H. Rulkens, and H. Bruning, "Photocatalyzed oxidation of alcohols and organochlorides in the presence of native TiO₂ and metallized TiO₂ suspensions. Part (I): photocatalytic activity and pH influence," *Water Research*, vol. 33, no. 3, pp. 661–668, 1999.
- [33] J. Chen, D. F. Ollis, W. H. Rulkens, and H. Bruning, "Photocatalyzed oxidation of alcohols and organochlorides in the presence of native TiO₂ and metallized TiO₂ suspensions. Part (II): photocatalytic mechanisms," *Water Research*, vol. 33, no. 3, pp. 669–676, 1999.
- [34] A. V. Vorontsov and V. P. Dubovitskaya, "Selectivity of photocatalytic oxidation of gaseous ethanol over pure and modified TiO₂," *Journal of Catalysis*, vol. 221, no. 1, pp. 102–109, 2004.
- [35] P. Ciambelli, D. Sannino, V. Palma, V. Vaiano, and R. S. Mazzei, "A step forwards in ethanol selective photo-oxidation," *Photochemical and Photobiological Sciences*, vol. 8, no. 5, pp. 699–704, 2009.
- [36] V. Vaiano, *Heterogeneous photocatalytic selective oxidation of cyclohexane*, Ph.D. thesis, University of Salerno, Salerno, Italy, 2006.
- [37] V. Palma, D. Sannino, V. Vaiano, and P. Ciambelli, "Fluidized-bed reactor for the intensification of gas-phase photocatalytic oxidative dehydrogenation of cyclohexane," *Industrial and Engineering Chemistry Research*, vol. 49, no. 21, pp. 10279–10286, 2010.
- [38] G. Colón, M. C. Hidalgo, and J. A. Navío, "Photocatalytic behaviour of sulphated TiO₂ for phenol degradation," *Applied Catalysis B: Environmental*, vol. 45, no. 1, pp. 39–50, 2003.
- [39] K. Okazaki, Y. Morikawa, S. Tanaka, K. Tanaka, and M. Kohyama, "Effects of stoichiometry on electronic states of Au and Pt supported on TiO₂(110)," *Journal of Materials Science*, vol. 40, no. 12, pp. 3075–3080, 2005.
- [40] M. C. Hidalgo, J. J. Murcia, J. A. Navío, and G. Colón, "Photodeposition of gold on titanium dioxide for photocatalytic phenol oxidation," *Applied Catalysis A: General*, vol. 397, no. 1-2, pp. 112–120, 2011.
- [41] C. D. Wagner, A. V. Naumkin, A. Kraut-Vass, J. W. Allison, C. J. Powell, and J. R. Rumble Jr., "NIST X-ray photoelectron spectroscopy database," <http://srdata.nist.gov/xps/>.
- [42] University of Leipzig, Leipzig, Germany, <http://www.zv.uni-leipzig.de/>.
- [43] J. Lee and W. Choi, "Photocatalytic reactivity of surface platinumized TiO₂: substrate specificity and the effect of Pt oxidation state," *Journal of Physical Chemistry B*, vol. 109, no. 15, pp. 7399–7406, 2005.
- [44] B. Llano, G. Restrepo, J. M. Marín, J. A. Navío, and M. C. Hidalgo, "Characterisation and photocatalytic properties of titania-silica mixed oxides doped with Ag and Pt," *Applied Catalysis A: General*, vol. 387, no. 1-2, pp. 135–140, 2010.



Hindawi

Submit your manuscripts at
<http://www.hindawi.com>

